Visual Salience-Guided Mesh Decomposition

Summary

Generally, decomposition is a leverage to obtain the componential representation from a whole. After the decomposition step is executed, the decomposed components can be individually selected, grouped, and analyzed based on the properties of interest. According to Hoffman and Singh's theory [1], there are at least three factors that determine the salience of a part: the protrusion, the boundary strength, and the relative size. However, the quantitative definitions for part salience proposed by Hoffman and Singh [1] were made under the assumption that a part and its boundary are found in advance. In this paper, we propose a new 3D mesh decomposition scheme that incorporates the psychological theory of visual salience, in such a way that the mesh decomposition process is as close as possible to the human visual perception mechanism.

Visual Salience-Guided Mesh Decomposition

A. Modeling the Protrusion as the Degree of Center

To characterize the protrusion of a part, we adopt the integral function described in [2]. Here, in contrast to [2], the integral function is constructed on the dual graph of a given mesh, $G = (V, E)$, where V and E represent the set of dual vertices and the set of dual edges, respectively. Let $area(v)$ denote the area occupied by a dual vertex v and $area(V)$ denote the total area of the object surface. The protrusion degree at a dual vertex v can be defined as [2]:

$$\mu(v) = \sum_i g(v, b_i) \cdot area(b_i), \qquad (1)$$

where $\{b_0, b_1, \ldots\}$ are the base dual-vertices, which are used to approximate the above integral function. In addition, $area(b_i)$ is the area of the base and $\sum_i area(b_i) = area(V)$.

Fig.1(a) shows the protrusion characterization of the dinopet model.

B. Choosing the Salient Representatives of Parts

Given a dual vertex $r \in V$, the dual vertex is chosen as a salient representative of a part if the following condition is satisfied:

$\Pr otrusion(r) = \max\{\Pr otrusion(v) \mid v \in V, g(r,v) < thr_p\}$, where thr_p represents the size of an observation window for finding a local maximum. Fig. 1(b) shows the six salient representatives of parts chosen from the dinopet model.

C. Modeling the Boundary Strength as the Border Area Change

For the purpose of clarity, we propose to split the computational process for modeling the boundary strength into two steps:

Step 1. Establishing the Candidate Locales: Given a salient representative of a part *r*, a set of candidate locales $\{L_r^x\} = \{L_r^0, L_r^1, ...\}$ is established using a modified version of the single-source Dijkstra's algorithm. For the purpose of simplicity and later use, we denote the x^{th} candidate locale as: $L^x = \{v \mid \forall v \in V, x \cdot e \le D(v) < (x+1) \cdot e\}$ for $x \in \{0,...,l-1\}$, where $D(v)$ returns the shortest distance from the source *r* to a dual vertex *v*, in terms of geodesic distance and protrusive difference. *e* represents the extent of a candidate locale, in which the boundary evolution is explored. *l* is the number of candidate locales. Figs. 1(c)-1(e) illustrate the construction of candidate locales, termination base, and constrained locales for the dinopet model.

Step 2. Modeling the Boundary Strength: With the constrained set of candidate locales established in Step 1, we now consider two adjacent locales in *L* to explore how the surface evolves in candidate locales. We propose to associate the following geometric property to the x^{th} candidate locale in *L*:

$$f(x) = \sum_{v \in V_{L^x}} area(v), \qquad (2)$$

Since V_{L^x} is a set of dual vertices that collects the direct neighbors between L_x and L_{x+1}, $f(x)$ can be regarded as the total-area-of-border between two adjacent candidate locales. Fig. 1(f) shows that the original function $f(x)$ shown in Fig. 1(j) was plotted on the surface of the dinopet model. Based on the geometric property defined in Eq. (2), we propose to model the boundary strength as the total-area-of-border change in response to the boundary evolution.

D. Finding the Locale of A Part Boundary

We propose to transform the function $f(x)$ into w different scales, $f_1(x)$, $f_2(x)$,…, $f_w(x)$. In this way, one can conduct a coarse-to-fine search for identifying the locale that contains a part boundary. Figs. 1(k)-1(m) shows three different scales of the original function, $f_1(x)$, $f_2(x)$, and $f_3(x)$, respectively. Their corresponding plots on the surface mesh were shown in Figs. 1(g)-1(i), respectively. As shown in Fig. 1(n), the locale of the boundary was formed by the union of the 11^{th}-13^{th} candidate locales. Fig. 1(o) shows that the nearly concave boundary can be generated from the locale shown in Fig. 2(n) by solving the maximum-flow problem [3].

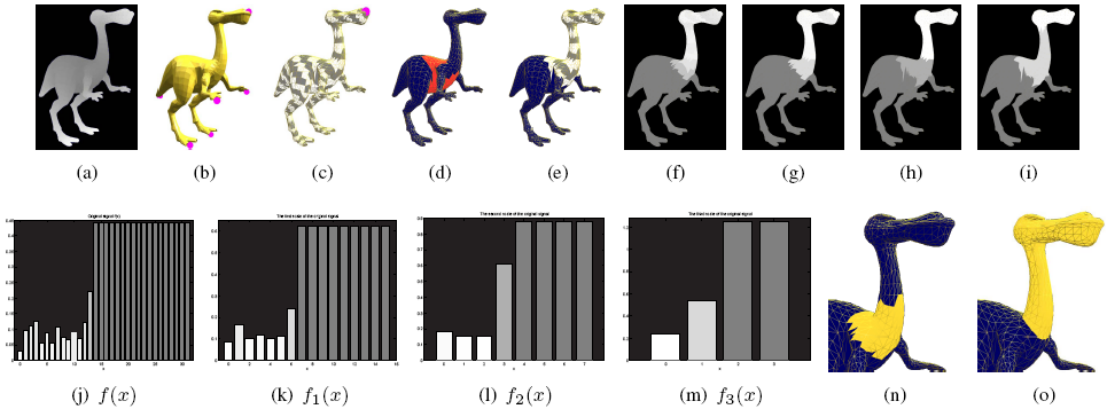

Fig 1. Illustration of (a) the protrusion characterization, (b) the salient representatives of parts, (c) the candidate locales, (d) the termination base, (e) the constrained candidate locales, (f)-(i) the different scaled versions of the function $f(x)$ plotted on the object surface, (j)-(m) the different scaled versions of the function $f(x)$, (n) the locale of a part boundary, and (o) the visual part and its boundary for the dinopet model.

Experimental Results

A series of experiments were conducted to test the effectiveness of the proposed method. Fig. 2 shows that the proposed method still succeeded in decomposing the dinopet models which were subject to the effects of different noise strengths on the randomization applied to the vertex coordinates.

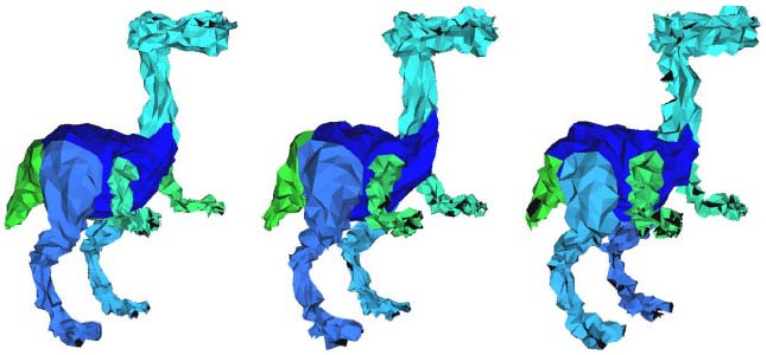

(a) ns=0.3 (b) ns=0.4 (c) ns=0.5

Fig. 2. The robustness of the proposed visual salience-guided mesh decomposition method under the randomization of vertex coordinates, which is controlled by means of the noise strength *ns* (i.e., the ratio of the largest displacement to the longest edge of the object's bounding box).

Hsueh-Yi Sean Lin[1,2], Hong-Yuan Mark Liao[1], and Ja-Chen Lin[2]

[1]Institute of Information Science, Academia Sinica

[2]Department of Computer Science, National Chiao-Tung University

References

1. D. D. Hoffman and M. Singh, (1997) *Cognition*, vol. 63, pp. 29-78.

2. M. Hilaga, Y. Shinagawa, T. Kohmura, and T. L. Kunii, (2001) *Proc. SIGGRAPH*, pp. 203-212.

3. S. Katz and A. Tal, (2003) *Proc. SIGGRAPH*, pp. 954-961.